ACS APPLIED MATERIALS & INTERFACES

Research Article

www.acsami.org

Highly Chemiluminescent Graphene Oxide Hybrids Bifunctionalized by *N*-(Aminobutyl)-*N*-(Ethylisoluminol)/Horseradish Peroxidase and Sensitive Sensing of Hydrogen Peroxide

Xiaoying Liu, Zhili Han, Fang Li, Lingfeng Gao, Gaolin Liang, and Hua Cui*

CAS Key Laboratory of Soft Matter Chemistry, Collaborative Innovation Center of Chemistry for Energy Materials, Department of Chemistry, University of Science and Technology of China, Hefei, Anhui 230026, P. R. China

Supporting Information

ABSTRACT: *N*-aminobutyl-*N*-ethylisoluminol and horseradish peroxidase bifunctionalized graphene oxide hybrids (ABEI-GO@HRP) were prepared through a facile and green strategy for the first time. The hybrids exhibited excellent chemiluminescence (CL) activity over a wide range of pH from 6.1 to 13.0 when reacted with H_2O_2, whereas ABEI functionalized GO had no CL emission at neutral pH and showed more than 2 orders of magnitude lower CL intensity than ABEI-GO@HRP at pH 13.0. Such strong CL emission from ABEI-GO@HRP was probably due to that HRP and GO facilitated the formation of $O_2^{\bullet-}$, $-CO_4^{\bullet 2-}$, $HO^{\bullet}$, and π-C=C$^{\bullet}$ in the CL reaction, and GO as a reaction interface promoted the electron transfer of the radical-involved reaction. By virtue of ABEI-GO@HRP as a platform, an ultrasensitive, selective, and reagentless CL sensor was developed for H_2O_2 detection. The CL sensor exhibited a detection limit of 47 fM at physiological pH, which was more than 2 orders of magnitude lower than previously reported methods. This work reveals that bifunctionalization of GO by ABEI and HRP leads to excellent CL feature and enzyme selectivity, which can be used as an ideal platform for developing novel analytical methods.

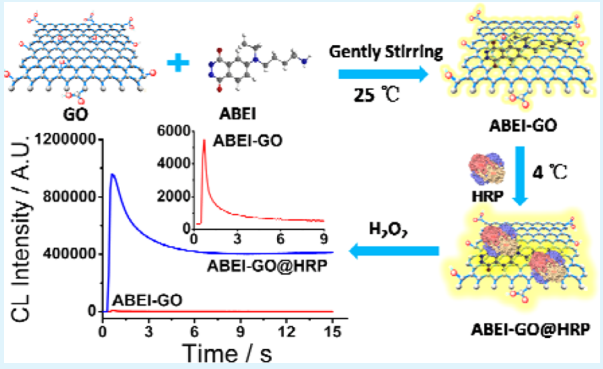

KEYWORDS: *horseradish peroxidase, N-(aminobutyl)-N-(ethylisoluminol), graphene oxide, chemiluminescence, sensor*

INTRODUCTION

Graphene oxide (GO), as a derivative of graphene, has attracted considerable interest in recent years for its remarkable properties, unique structural features, and ease of fabrication.[1−3] The incredibly large specific surface area (two accessible sides), abundant oxygen-containing surface functionalities, and high water solubility make GO sheets an ideal matrix for constructing novel hybrid materials with new features.[4,5] To date, a series of functionalized GO hybrid materials with highly effective surface area, photoactivity, electroactivity, chemical stability, and biocompatibility have been successfully synthesized.[6,7] However, few studies have been reported regarding GO sheets with novel chemiluminescence (CL) and electrochemiluminescence (ECL) properties. Recently, GO hybrid materials noncovalently functionalized by CL reagents with aromatic rings such as lucigenin, luminol, and *N*-(aminobutyl)-*N*-(ethylisoluminol) (ABEI) have been successfully synthesized by our group via facile synthesis strategies and exhibited good CL activity, stability, and biocompatibility.[8−11] After introducing a catalyst hemin,[12] CL reagent ABEI and catalyst hemin bifunctionalized GO hybrids (ABEI-hemin-GNs) with greatly improved CL activity were obtained. However, the synthesized ABEI-hemin-GNs were purified by dialysis for more than 2 days, which was tedious and time-consuming. And the ABEI-hemin-GNs hybrids are difficult to further conjugate with recognition biomolecules such as single strand DNA and antibodies due to multilayer stacking on the surface of graphene, limiting their applications in sensors. Moreover, the analytical application of the ABEI-hemin-GNs hybrids has not been explored. Therefore, it is very important to explore GO hybrids bifunctionalized by CL reagents and other catalysts in order to achieve excellent CL activity, as well as other physical and chemical features and to develop highly sensitive and selective sensors.

As a prototypical peroxidase, horseradish peroxidase (HRP) is often used as a catalyst of the luminol−H_2O_2 reaction[13] for the amplified CL or ECL detection of DNA, metal ions, biomolecules, and hydrogen peroxide or related compounds.[14,15] Although HRP is identified as a popular catalyst for the CL reaction, its applications are often limited by its lack of long-term stability and difficulties in recovery and recycling in aqueous reaction.[16] In recent years, HRP immobilization has been proven an efficient way to overcome the problems mentioned above. GO, attributing to its abundant oxygen-

Received: April 9, 2015
Accepted: July 31, 2015
Published: July 31, 2015

DOI: 10.1021/acsami.5b05325
ACS Appl. Mater. Interfaces 2015, 7, 18283−18291

Scheme 1. Fabrication of ABEI-GO@HRP

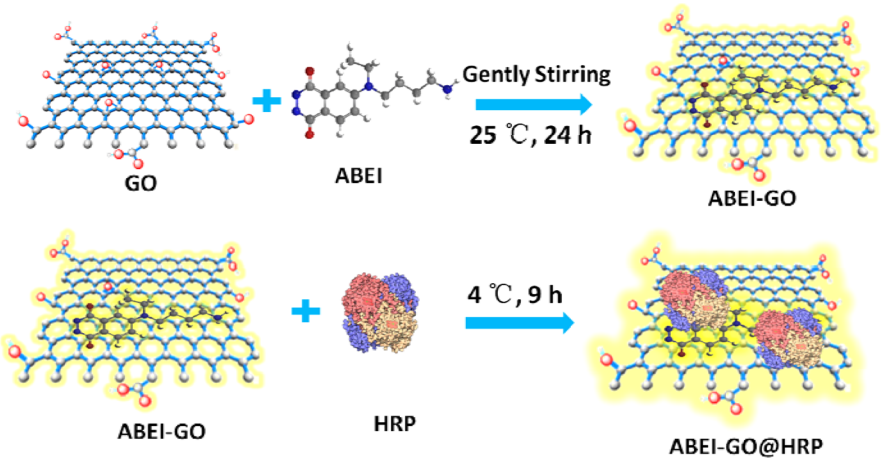

containing groups, such as epoxide, hydroxyl, and carboxylic groups, is considered to be an ideal platform for immobilizing HRP via covalent and/or noncovalent binding without any surface modification or coupling reagents.[17−19] Owing to the hydrophilic and biocompatible microenvironment afforded by GO, the immobilized HRP on the surface of GO possess several advantages over the free one, such as high-thermal and storage stability and easy separation from the reaction mixture.[20] Therefore, the immobilized HRP can find more practical applications in biocatalysis, biosensors, and biotechnology.[21] We suppose that if both the CL reagent and HRP are simultaneously modified on the surface of GO sheets, the hybrid materials with unique CL features and enzymatic activity might be obtained.

In this work, ABEI (as a CL reagent model) and HRP bifunctionalized GO hybrids (ABEI-GO@HRP) were successfully synthesized by virtue of self-assembly interaction among ABEI, HRP, and GO. The as-prepared ABEI-GO@HRP hybrids were characterized by X-ray photoelectron spectroscopy (XPS), Fourier transform infrared spectroscopy (FT-IR), transmission electron microscopy (TEM), atomic force microscopy (AFM), and circular dichroism (CD) spectroscopy. The assembling mechanism was investigated. The CL behavior of the as-prepared ABEI-GO@HRP hybrids in liquid phase was explored in alkaline and neutral conditions. It was found that ABEI-GO@HRP hybrids exhibited excellent CL activity when reacted with H_2O_2 both in alkaline and neutral conditions. The CL mechanism of ABEI-GO@HRP has been proposed by studying the effect of O_2 and radical scavengers. Finally, by virtue of ABEI-GO@HRP as a platform, a selective and reagentless sensor for the sensitive detection of H_2O_2 in physiological pH and alkaline conditions was developed. To the best of our knowledge, this is the most sensitive sensor for the detection of H_2O_2 at physiological pH and alkaline conditions.

EXPERIMENTAL SECTION

Chemicals and Materials. GO was purchased from XFNANO Materials Tech Co., Ltd. (Nanjing, China). ABEI was obtained from Sigma-Aldrich (U.S.A.), and a stock solution of ABEI (0.01 M) was prepared by dissolving ABEI in NaOH solution (0.1 M). HRP (R_z > 3.0) was purchased from Shanghai Sangon Biotechnology Co., Ltd. (Shanghai, China). Working solutions of H_2O_2 were prepared fresh daily from 30% (v/v) H_2O_2 (Xinke Electrochemical Reagent Factory, Bengbu, China). All other reagents were of analytical grade. Ultrapure water was prepared by a Milli-Q system (Millipore, France) and used throughout.

Synthesis and Characterization of ABEI-GO@HRP. A schematic illustration for the synthesis of ABEI-GO@HRP hybrids is shown in Scheme 1. First, 500 μL of 0.01 M ABEI alkaline solution was added into 50 mL of 0.1 mg/mL homogeneous GO dispersion and stirred gently at room temperature for 24 h until the color from pale-yellow to dark brown unchanged, indicating that ABEI functionalized GO composites (ABEI-GO) were successfully synthesized. The resulting solution was centrifuged twice at a speed of 13 000 rpm for 15 min to remove residual ABEI and redispersed in isopyknic disodium hydrogen phosphate-citrate (D-C, 10 mM, pH = 5.6) buffer. Then 1 mg/mL HRP dissolved in pH 5.6 D-C buffer was added into the redispersed solution above by the volume ratio at 1:10 of HRP and ABEI-GO and was incubated at 4 °C for 9 h. After centrifuging to remove nonspecifically adsorbed enzyme and redispersing in ultrapure water, ABEI-GO@HRP hybrids were obtained. The as-synthesized ABEI-GO and ABEI-GO@HRP hybrids were subsequently characterized by XPS, FT-IR, TEM, AFM, and CD spectra.

CL Measurements. CL measurements were conducted on a Centro LB 960 microplate luminometer (Berthold, Germany). For a typical CL measurement, 50 μL of ABEI-GO@HRP and other control substances were added into each well of microplate, respectively, then 50 μL of 100 μM H_2O_2 solution dissolving in 0.1 M NaOH (pH = 13.0), 10 mM Britton-Robinson (B-R), 10 mM D-C, 10 mM Tris-HCl, 10 mM borate, or 10 mM phosphate buffer solutions was injected into each well. The light emission was collected by the microplate luminometer. The CL spectrum was measured on a model F-7000 spectrofluorophotometer with the excitation source off.

H_2O_2 Detection. For a typical experiment, 50 μL of H_2O_2 with different concentrations in 0.1 M NaOH solution (pH 13.0) or 10 mM D-C buffer solution (pH 8.0) was injected into the microwell of 96-well plates with 50 μL aqueous dispersion of the as-prepared ABEI-GO@HRP hybrids, and then the CL kinetic curves were recorded immediately. To investigate the selectivity of the sensor at pH 8.0, various interferents that can be found in biological media and can serve as substrate for HRP, including ascorbic acid, dopamine, urea peroxide, *p*-aminophenol, nicotinamide-adenine dinucleotid (NADH), and tyrosine, were measured instead of H_2O_2. When the CL sensor was used to determine H_2O_2 in human urine samples, freshly voided human urine samples were collected from healthy volunteers. Before the measurements, the urine samples were deproteinized by ultrafiltration (3000 Da cutoff), followed by 10 000 times dilution with 10 mM D-C buffer (pH 8.0) and 60 min store.

RESULTS AND DISCUSSION

Synthesis and Characterization of ABEI-GO@HRP. The synthesis of ABEI-GO@HRP hybrids is illustrated in Scheme 1. To start with, the mixture of ABEI solution and GO dispersion

DOI: 10.1021/acsami.5b05325
ACS Appl. Mater. Interfaces 2015, 7, 18283−18291

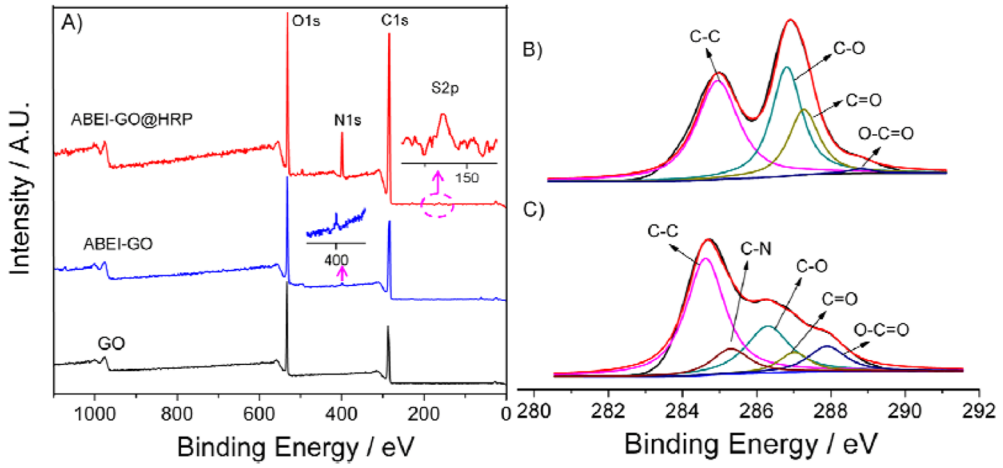

Figure 1. Survey XPS data A) of GO, ABEI-GO, and ABEI-GO@HRP. The deconvolution of C 1s spectra of B) GO and C) ABEI-GO@HRP. The insets are the magnification of N 1s in ABEI-GO and S 2p in ABEI-GO@HRP, respectively.

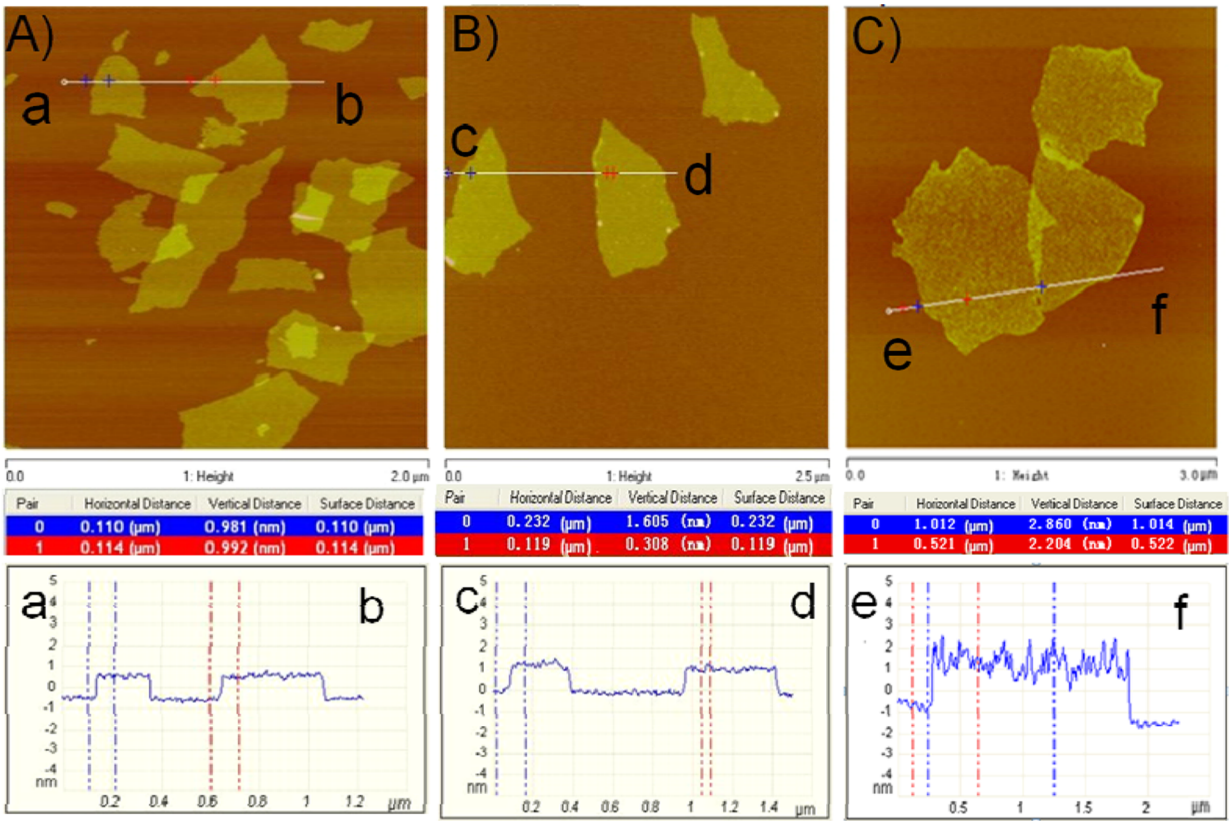

Figure 2. Tapping mode AFM images of A) exfoliated GO, B) ABEI-GO, and C) ABEI-GO@HRP.

were gently stirred at room temperature for 24 h to prepare ABEI-GO. Then 1 mg/mL of HRP was added into the as-prepared ABEI-GO aqueous solution, and the mixture was incubated at 4 °C for 9 h. After centrifugation, ABEI-GO@HRP hybrids were obtained.

The composition of the as-prepared ABEI-GO@HRP hybrids was investigated by XPS, FT-IR, and CD spectra. XPS results are shown in Figure 1. Comparing survey XPS (Figure 1A) of ABEI-GO with that of GO, there was a new component of N 1s at 398.5 eV, indicating the existence of ABEI molecules and/or their oxidation products on the surface of ABEI-GO composites. The immobilization of HRP resulted in a significant increase in N 1s peak and a new peak at ~164.05 eV attributed to sulfur S 2p,[22] as shown in Figure 1A, supporting the presence of HRP. In addition, the weight ratio of carbon to oxygen in ABEI-GO was 1.79, which was higher than that of GO (1.42) but much lower than that of graphene (3.13), showing that GO in ABEI-GO was partly reduced. Furthermore, comparing the C 1s spectrum of ABEI-GO@HRP composites with that of GO, as shown in Figure 1B, 2C, a new peak at 285.2 eV corresponding to C—N was observed, which strongly supported that ABEI or HRP existed on the surface of GO. Peaks at 284.6 eV, 286.4 eV, 287.2, and 288.2 eV in ABEI-GO@HRP (Figure 3C) suggested the existence of C—C, C—O, C═O, and O—C═O.

DOI: 10.1021/acsami.5b05325
ACS Appl. Mater. Interfaces 2015, 7, 18283−18291

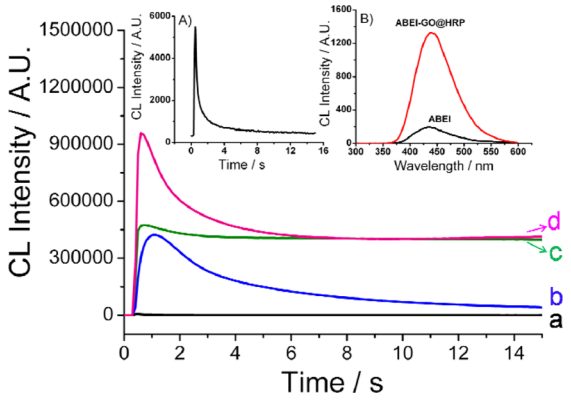

Figure 3. A comparison of CL behavior for ABEI-GO (curve a), ABEI-GO + 2.2 μg HRP (curve b), ABEI-hemin-GNs (curve c), and ABEI-GO@HRP (curve d) in alkaline conditions. The inset A) is the magnification of ABEI-GO. The inset B) is the CL spectra of ABEI and ABEI-GO@HRP. Reaction condition: 100 μM H_2O_2 in 0.1 M NaOH solution.

The presence of ABEI and HRP molecules on the surface of ABEI-GO@HRP was also confirmed by FT-IR spectrum. As shown in Supporting Information (SI) Figure S1, after being functionalized by ABEI and HRP, FT-IR spectrum of ABEI-GO@HRP demonstrated a typical amino group band of ABEI (3341 cm^{-1}), amide I (1654 cm^{-1}), and amide II (1535 cm^{-1}) infrared absorption bands of HRP.[23] The existence of active HRP on the surface of ABEI-GO@HRP was demonstrated by CD spectra. Generally, most of the biomacromolecules can be observed in CD spectra for its chirality.[24] However, GO is a kind of two-dimensional material without chirality and thus cannot be observed in CD spectra.[25] Therefore, CD spectroscopy can be a good assistant method to ascertain the immobilization of HRP on the surface of ABEI-GO. As shown in Figure S2, the HRP and ABEI-GO@HRP composite had an optically active band in CD spectra except GO, revealing that HRP was assembled on the surface of ABEI-GO successfully without denaturation. Therefore, we could conclude that both ABEI and HRP were successfully functionalized on the surface of GO.

The morphology and thickness of the as-prepared ABEI-GO@HRP composite were studied by AFM and TEM. From the AFM images shown in Figure 2, the thickness of exfoliated GO sheet is about 1 nm, demonstrating a single atomic layer thickness structure feature.[26,27] After being functionalized with ABEI, the height of ABEI-GO shows a 0.6 nm increment, indicating that monolayer ABEI molecules are attached to both sides of GO via $\pi-\pi$ stacking, which is in good agreement with our previous work.[8,12] Owing to the immobilization of HRP, the mean thickness of ABEI-GO@HRP increased 1.2 nm, and HRP particles distributed uniformly on the surface of ABEI-GO@HRP, which is in good agreement with a 1.2 nm increment when HRP was directly immobilized on the surface of GO as shown in Figure S3A, S3B. The results indicated that HRP may be adsorbed on both sides of the as-prepared ABEI-GO in a monolayer. The morphology of ABEI-GO@HRP was also characterized by TEM. The specimen of TEM was prepared by dropping the sample onto a copper net covered by a carbon film. As the solvent was evaporated, wrinkles appeared for GO under a surface tension effect, as shown in Figure S4A. After the immobilization of HRP as shown in Figure S4B, the ABEI-GO material dispersed easily on the carbon film, demonstrating the changes in surface characteristics of the composite. And the loading of HRP on GO was calculated to be 0.455 g HRP per g GO using UV−visible absorption spectra. The detailed calculation process is described in the SI.

CL Activity of ABEI-GO@HRP. HRP has been intensively utilized to enhance CL of the luminol-H_2O_2 system.[28] ABEI is an analogue of luminol. Considering the fact that ABEI-GO@HRP hybrids contain CL reagent ABEI molecules and catalyst HRP, ABEI-GO@HRP hybrids might have excellent CL activity. Accordingly, the CL behavior of ABEI-GO@HRP hybrids was studied by static injection on a microplate luminometer in typical alkaline solution in which strong CL emission was often obtained for luminol-type CL reagents[29,30] as shown in Figure 3. When 50 μL of 100 μM H_2O_2 alkaline solution (pH = 13.0) was injected to 50 μL of ABEI-GO@HRP aqueous solution in a microwell, more than 2 orders of magnitude (174 times) higher CL emission than ABEI-GO under the same conditions was observed. Although the CL intensity of ABEI-GO also increased after the addition of free HRP (the same amount as HRP on the surface of ABEI-GO@HRP), its CL intensity was still 3.5 times weaker than that of ABEI-GO@HRP. The CL behavior of ABEI-GO@HRP was also compared with our previously synthesized ABEI-hemin-GNs. ABEI-GO@HRP exhibit around 3 times higher CL intensity than ABEI-hemin-GNs. The CL spectra of ABEI-GO@HRP-H_2O_2 system showed a peak centered at 440 nm as shown in Figure 3, inset B, which was in accordance with that of the CL reaction of ABEI and H_2O_2. The result revealed that

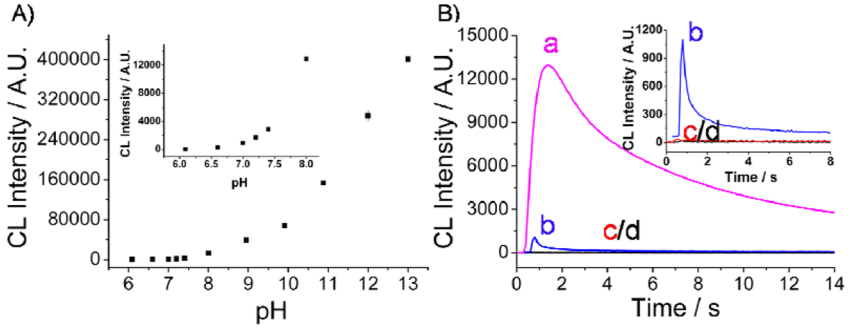

Figure 4. A) The effect of pH of H_2O_2 on the CL intensity of ABEI-GO@HRP. Reaction conditions: 50 μL 10 μM H_2O_2 in B-R buffer (pH 6.1−11.2) and NaOH solution (pH 12.0−13.0) was injected into 50 μL ABEI-GO@HRP water dispersion in a microwell. Insert: magnification of curves of pH from 6.1 to 8.0. B) CL kinetic curves for reactions of a) ABEI-GO@HRP at pH 8.0, b) ABEI-GO at pH 13.0, c) 0.1 mM ABEI at pH 8.0, and (d) ABEI-GO at pH 8.0 in the presence of 10 μM H_2O_2. Inset: magnification of curves of b, c and d.

DOI: 10.1021/acsami.5b05325
ACS Appl. Mater. Interfaces 2015, 7, 18283−18291

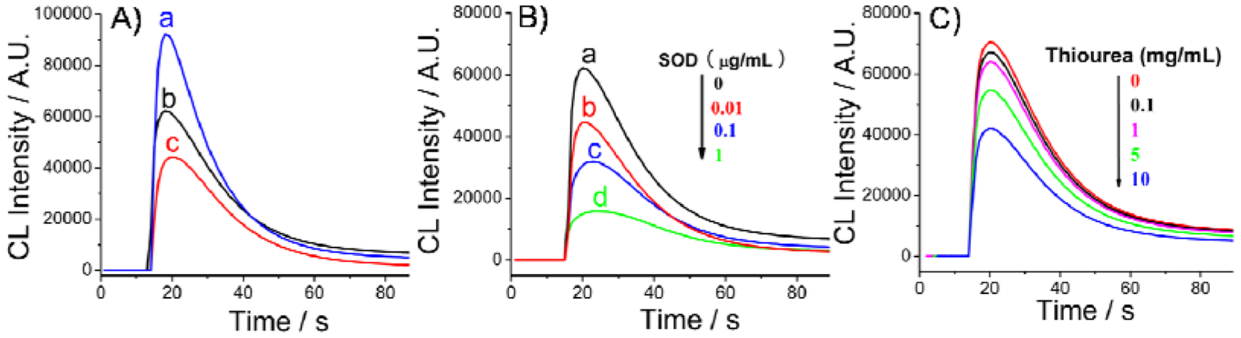

Figure 5. A) CL kinetic curves of ABEI-GO@HRP-H_2O_2 under oxygen-saturated (a), air-saturated (b) and nitrogen-saturated solutions (c), respectively; B) CL kinetic curves of ABEI-GO@HRP-H_2O_2 in the absence (a) and presence of different concentrations of SOD: 0.01 μg/mL (b), 0.1 μg/mL (c), 1 μg/mL (d); C) CL kinetic curves of ABEI-GO@HRP-H_2O_2 in the absence (black line) and presence of different concentrations of thiourea: 0.1 mg/mL (black line), 1 mg/mL (pink line), 5 mg/mL (green line), and 10 mg/mL (blue line). Reaction conditions: 50 μL 1 μM H_2O_2 in 0.1 M NaOH was injected into 50 μL ABEI-GO@HRP aqueous solutions; Voltage of PMT was set at 700 V.

the CL emission resulted from the reaction of ABEI molecules on the surface of ABEI-GO@HRP with H_2O_2.

Effect of pH on CL Activity. In order to further study the CL activity of ABEI-GO@HRP hybrids and excavate its possible application potential, the effect of the pH of H_2O_2 on the CL intensity of ABEI-GO@HRP hybrids was studied. As shown in Figure 4A. 10 μM H_2O_2 with different pH values were obtained by diluting H_2O_2 with B-R buffer (pH 6.1−11.2) and NaOH solution (pH 12.0−13.0). The CL intensity increased sharply with increasing the pH, which is in good agreement with earlier studies because more intermediate radicals are produced at high pH.[31,32] As shown in Figure 4A and 4B, it is worth noting that ABEI-GO@HRP hybrids still exhibited good CL activity in the pH ranges of 7.0−8.0, whereas almost no CL emission was observed for 0.1 mM ABEI solution used for synthesis and ABEI-GO, indicating that the catalytic activity of HRP immobilized on ABEI-GO plays a major role in the decomposition of H_2O_2 in physiological conditions. Moreover, the CL emission of ABEI-GO@HRP at pH 8.0 is even more than 1 order of magnitude higher than ABEI-GO at pH 13.0. Such a strong CL of ABEI-GO@HRP provides application possibility under physiological conditions.

Proposed CL Mechanism. The excellent CL efficiency of ABEI-GO@HRP hybrids may be due to good catalytic effect of the immobilized HRP and the effect of GO. Our previous work has proposed that the CL catalysis and enhancement of the ABEI-H_2O_2 system related to the generation of oxygen-related radicals such as $HO^{\bullet}$ and $O_2^{\bullet-}$ and an improved electron transfer.[33] Earlier studies showed that HRP as an oxidoreductase could catalyze the decomposition of H_2O_2 to form a reactive complex, followed by the reaction with luminol to produce luminol radicals, accelerating the CL reaction.[28] ABEI, an analogue of luminol, may follow a similar mechanism to trigger the oxidation of ABEI anions ($ABEI^-$) to produce ABEI radicals ($ABEI^{\bullet-}$). Recent studies demonstrated that the catalytic efficiency of HRP immobilized on the surface of GO could be improved.[16] Moreover, GO as a nanosized platform could facilitate radical generation and electron transfer in chemical reactions.[34−36] Therefore, excellent CL activity of ABEI-GO@HRP hybrids might be due to the fact that HRP and GO facilitate radical generation and GO as a reaction platform stimulates electron transfer in radical-involved CL reaction, accelerating the CL reaction. To confirm the CL mechanism, the effect of O_2 and the radical scavengers on the CL intensity was investigated by static injection. As shown in Figure 5A, the CL intensity decreased in a nitrogen-saturated solution and increased in an oxygen-saturated solution, indicating that the dissolved oxygen (O_2) was indispensable for this CL system. It was reported that $ABEI^{\bullet-}$ produced by HRP catalysis and GO could facilitate the conversion of dissolved oxygen to $O_2^{\bullet-}$.[28,34] And $O_2^{\bullet-}$ could react with H_2O_2 to produce $HO^{\bullet}$.[37] $O_2^{\bullet-}$ and $HO^{\bullet}$ were important intermediate radicals for ABEI CL reaction. To identify the radical species, the effect of radical scavengers superoxide dismutase (SOD) and thiourea of $O_2^{\bullet-}$ and $HO^{\bullet}$ on the CL intensity was studied. As shown in Figure 5B, the CL intensity decreased with increasing the concentrations of SOD, demonstrating that $O_2^{\bullet-}$ was involved in the CL reaction. Similarly, the CL intensity also decreased with increasing the concentrations of thiourea as shown in Figure 5C, indicating that $HO^{\bullet}$ was related to the CL reaction. These results showed that both $O_2^{\bullet-}$ and $HO^{\bullet}$ were participating in the reaction of ABEI-GO@HRP-H_2O_2. A recent study showed that $HO^{\bullet}$ would immediately add to double bonds at the GO plane to form strongly oxidizing π-conjugated carbon radicals (π-C═C$^{\bullet}$), which could initiate the long-lasting visible CL of luminol in alkaline condition.[38] Therefore, $HO^{\bullet}$ might simultaneously add to double bonds at the GO plane to generate π-C═C$^{\bullet}$ radicals, which then reacted with $ABEI^-$, accelerating the production of $ABEI^{\bullet-}$. It has been reported that $O_2^{\bullet-}$ could react with $-COO^-$ groups in 2-[bis[2-[carboxymethyl-[2-oxo-2-(2-sulfanylethylamino)ethyl]-amino]ethyl]amino]acetic acid (DTDTPA) to form $-CO_4^{\bullet 2-}$, which could react with $ABEI^-$ to facilitate the formation of $ABEI^{\bullet-}$.[33] Thus, GO, owing to its enriched oxygen functional groups, especially for carboxyl groups, may contribute to such strong light emission of ABEI-H_2O_2 to some extent. To verify this speculation, the effect of GO, HRP, and GO@HRP on ABEI-H_2O_2 CL system was investigated as shown in Figure S5. The results indicated that GO, HRP, and GO@HRP complexes could catalyze the CL reaction to some extent, but their catalytic ability was much weaker than ABEI-GO@HRP hybrids. Overall, ABEI-GO@HRP hybrids facilitated the generation of several radicals such as $ABEI^{\bullet-}$, $O_2^{\bullet-}$, $HO^{\bullet}$, π-C═C$^{\bullet}$, and $-CO_4^{\bullet 2-}$. Finally, $ABEI^{\bullet-}$ further reacted with $O_2^{\bullet-}$ on the surface of GO to produce excited-state oxidation product *N*-(aminobutyl)-*N*-(ethyl phthalate) (ABEI-ox*), accompanying by strong light emission. The possible CL reaction pathways may be as eqs 1−14:

$$H_2O_2 + \text{HRP} \rightarrow \text{compound I} + H_2O \quad (1)$$

DOI: 10.1021/acsami.5b05325
ACS Appl. Mater. Interfaces 2015, 7, 18283−18291

$$\text{compound I} + \text{ABEI}^- \rightarrow \text{compound II} + \text{ABEI}^{\bullet -} + \text{H}_2\text{O} \quad (2)$$

$$\text{compound II} + \text{ABEI}^- \rightarrow \text{HRP} + \text{ABEI}^{\bullet -} \quad (3)$$

$$\text{ABEI}^{\bullet -} + \text{O}_2 \rightarrow \text{ABEI} + \text{O}_2^{\bullet -} \quad (4)$$

$$\text{O}_2^{\bullet -} + \text{H}_2\text{O}_2 \rightarrow \text{OH}^{\bullet} + \text{OH}^- + \text{O}_2 \quad (5)$$

$$\text{O}_2 \xrightarrow{\text{GO}} \text{O}_2^{\bullet -} \quad (6)$$

$$\text{H}_2\text{O}_2 \xrightarrow{\text{GO}} \text{OH}^{\bullet} + \text{O}_2^{\bullet -} \quad (7)$$

$$\text{OH}^{\bullet} + \text{GO} \rightarrow \pi\text{-C}{=}\text{C}^{\bullet} \quad (8)$$

$$\text{O}_2^{\bullet -} + \text{GO} \rightarrow \pi\text{-C}{=}\text{C}^{\bullet} \quad (9)$$

$$\pi\text{-C}{=}\text{C}^{\bullet} + \text{ABEI}^- \rightarrow \pi\text{-C}{=}\text{C} + \text{ABEI}^{\bullet -} \quad (10)$$

$$\text{O}_2^{\bullet -} + -\text{COO}^- \rightarrow -\text{CO}_4^{\bullet 2-} \quad (11)$$

$$-\text{CO}_4^{\bullet 2-} + \text{ABEI}^- \rightarrow \text{ABEI}^{\bullet -} \quad (12)$$

$$\text{ABEI}^{\bullet -} + \text{O}_2^{\bullet -} \xrightarrow{\text{GO}} \text{ABEI-ox*} \quad (13)$$

$$\text{ABIE} - \text{ox*} \rightarrow \text{ABEI} + h\nu \quad (14)$$

Detection of H_2O_2. H_2O_2 plays a critical role in a wide variety of signaling transduction processes, such as an oxidative stress marker in aging and disease, a defense agent in response to pathogen invasion.[39−41] It is believed that excessive H_2O_2 production is implicated with various diseases including cancer, diabetes, and cardiovascular and neurodegenerative disorders.[42,43] Therefore, simple, sensitive, and highly specific sensors for the detection of H_2O_2 are highly desired. As mentioned above, the as-synthesized ABEI-GO@HRP hybrids exhibited excellent CL activity when reacted with hydrogen peroxide. Accordingly, ABEI-GO@HRP hybrids could be directly used as a reagentless and sensitive sensor for hydrogen peroxide. Under the optimal conditions (1 mg/mL HRP in pH 5.6 disodium hydrogen phosphate-citrate (D-C) buffer, 9 h incubation time and 10 mM D-C buffer at pH 8.0 for H_2O_2) as shown in Figure S6, working curve for determination of H_2O_2 in D-C buffer solution at pH 8.0 is shown in Figure 6A. The CL intensity increased linearly with the logarithm of the concentration of H_2O_2 in the range of 0.1 pM to 10 nM. The regression equation was $I = 6536.9 + 453.47 \times \log C$ with a correlation coefficient of 0.997, where I refers to CL intensity and C the concentration of H_2O_2. The limit of detection (LOD) for H_2O_2 was 47 fM (LOD is defined as the concentration corresponding to bank signal $+3\sigma$, σ is the standard deviation of blank), which was more than 2 orders of magnitude lower than the best sensor reported so far.[44,45] For a comparison, the analytical performance of the sensor was also studied for the detection of H_2O_2 at pH 13.0. The results (Figure 6B) showed that the linear range and LOD is 1.0 pM to 10 nM and 0.30 pM, respectively. The limit of detection for H_2O_2 at pH 13.0 was also more than 1 order of magnitude lower than the best sensor reported so far. Attributing to the excellent CL performance of ABEI-GO@HRP, the dynamic linear ranges and detection limits of the present CL sensor demonstrate a great improvement over previously reported methods as listed in Table 1. It could be found that the detection limit at pH 13.0 is higher than that at pH 8.0 due to poor signal-to-background at pH 13.0. The relative standard deviation (RSD) of seven replicate detections of 10 nM H_2O_2 at pH 8.0 and pH 13.0 within a day was 1.28% and 1.86%, respectively, indicating good repeatability of the proposed H_2O_2 sensor. The selectivity of CL sensor toward H_2O_2 at pH 8.0 was also examined. As shown in Figure 7, various substrates of HRP, including ascorbic acid, dopamine, urea peroxide, *p*-aminophenol, nicotinamide-adenine dinucleotid (NADH), and tyrosine as interfering species, were measured instead of H_2O_2. H_2O_2 exhibited strong CL signal, whereas other species showed weak CL signal. The results demonstrate that the present CL sensor is selective toward H_2O_2 at physiological pH owing to the HRP specificity.

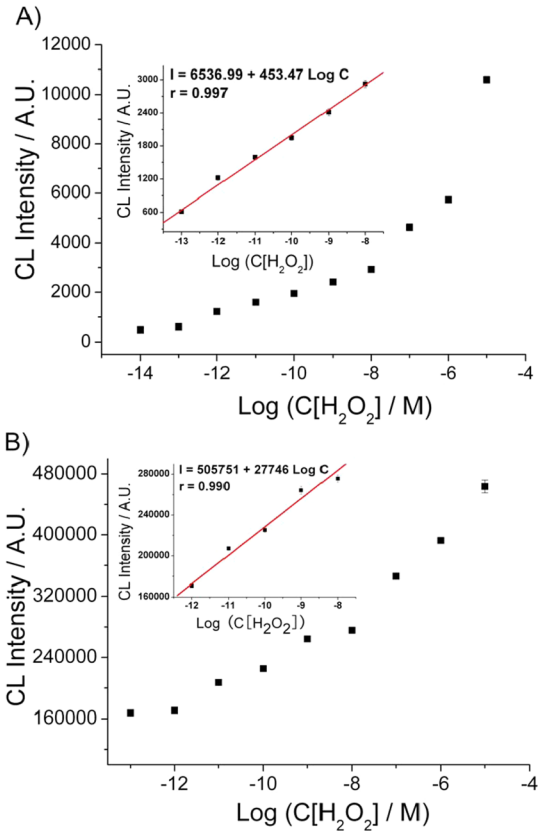

Figure 6. Calibration curves for H_2O_2 detection A) in D-C buffer solution (10 mM, pH 8.0) and B) in 0.1 M NaOH solutions (pH 13.0).

The potential applicability of the CL sensor for the detection of H_2O_2 in practical samples was also investigated by determining H_2O_2 in human urine samples. It has been reported that the quantification of H_2O_2 in urine might be a valuable biomarker of the extent of oxidative stress in vivo.[50] Prior to the determination, deproteinization of the urine samples with ultrafiltration was carried out to eliminate the possible effect of macromolecular proteins on the CL responses. H_2O_2 in human urine samples was determined as shown in Table 2. The concentration of H_2O_2 in tested normal human urine was in the range of 21.7−48.9 μM, which is in good agreement with the data obtained by literature.[51] The results show that the CL sensor is reliable. The recovery of H_2O_2 ranged from 96 to 103%, demonstrating that the CL sensor is applicable to monitor H_2O_2 in the practical human urine samples.

Assembling Mechanism of ABEI-GO@HRP. The assembling mechanism of ABEI-GO@HRP was explored by studying

DOI: 10.1021/acsami.5b05325
ACS Appl. Mater. Interfaces 2015, 7, 18283−18291

Table 1. Comparison of Proposed H_2O_2 Sensor with Previously Reported Sensors Based on HRP

H_2O_2 sensor	method	linear range (M)	LOD	ref
HRP-NCD	CM[a]	$3.9 \times 10^{-9} - 4.0 \times 10^{-3}$	35 nM	22
HRP-AuNCs	FL[b]	$1.0 \times 10^{-7} - 1.0 \times 10^{-4}$	30 nM	46
HRP-nanochannel	CV[c]	nM−μM	10 nM	47
$FcC_{11}SH$/encapsulated HRP	CV	$1.0 \times 10^{-9} - 1.6 \times 10^{-6}$	0.64 nM	48
HRP/AuNPs/CdTe-CdS/G-AuNP/GE	CV	$1.0 \times 10^{-10} - 1.2 \times 10^{-8}$	32 pM	49
HRP-nitrocellulose membranes	CL	$2.5 \times 10^{-11} - 1.5 \times 10^{-8}$	25 pM	44
amplex red-mediated SWV immobilized HRP	SWV[d]	$8.0 \times 10^{-12} - 3.0 \times 10^{-10}$	8 pM	45
ABEI-GO@HRP (pH = 8.0)	CL	$1.0 \times 10^{-13} - 1.0 \times 10^{-8}$	47 fM	this work
ABEI-GO@HRP (pH = 13.0)	CL	$1.0 \times 10^{-12} - 1.0 \times 10^{-8}$	0.30 pM	this work

[a]Colorimetric. [b]Fluorescence. [c]Cyclic Voltammetry. [d]Square Wave Voltammetry.

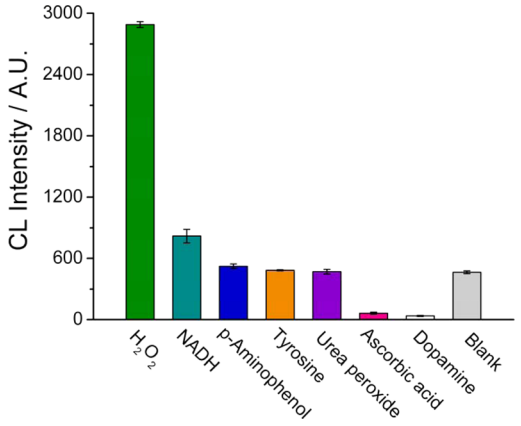

Figure 7. CL response of the proposed sensor to H_2O_2 and interferents (100 nM). Reaction conditions: 50 μL 10 nM H_2O_2 or various interferents in 10 mM D-C buffer solution (pH 8.0) was injected into 50 μL ABEI-GO@HRP water dispersion.

the interaction among GO, ABEI, and HRP. The pH of HRP solutions influencing the charge of HRP (pI = 7.2) played an important role in the immobilization of HRP. As shown in Figure S6A, when the pH of HRP solutions increased from 5.6 to 8.0, positively charged HRP became negatively charged HRP, and only a ~ 40% decrease in CL intensity was observed. In this case, negatively charged ABEI-GO (the z-potential of the ABEI-GO was −37.7 mV) should not be connected with negatively charged HRP at pH 8.0 and much more decrease in CL intensity should be observed because CL emission of ABEI-GO was only 0.6% of total CL emission if electrostatic bonding was only interaction between ABEI-GO and HRP. The result suggested that not only electrostatic interaction, but also other interactions such as $\pi-\pi$ stacking and hydrogen bonding might also contribute to the interactions because GO, ABEI, and HPR have aromatic rings, oxygen-containing groups, and amino acid residues. The AFM image of ABEI-GO@HRP (Figure 2C) demonstrates that there are two thicknesses, 2.8 and 2.2 nm, which both exhibit a 1.2 nm increment compared with that of ABEI-GO and GO, respectively. Therefore, it is suggested that two modes are involved in the HRP immobilization. The first one is that HRP and ABEI may be directly assembled on the surface of GO by strong electrostatic interaction and $\pi-\pi$ stacking, respectively, to form a thickness of 2.2 nm. Another possible mode is that HRP might be immobilized on the surface of ABEI-GO by using ABEI as a bridge molecule to form a thickness of 2.8 nm. In order to determine the interaction between HRP and ABEI, the quenching effect of HRP on fluorescence (FL) of ABEI and UV−vis spectroscopy were conducted. For the FL quenching experiment, various concentrations of HRP, ranging from 0 to 2.5 μM, were added into 10 μM ABEI solution in excess. As shown in Figure S7, with increasing HRP concentration, the FL intensity of ABEI (440 nm) gradually decreased. Furthermore, UV−vis experiment (Figure S8) revealed that absorbance sum of ABEI and HRP was not equal to the absorbance of the mixture of ABEI and HRP with the same concentration. These results demonstrated that ABEI molecules could interact with HRP molecules. According to Zhang's study[21] and our previous work,[12] there might be three possible interactions between HRP and ABEI molecule: the first one is $\pi-\pi$ stacking between the aromatic ring of ABEI and π-orbital-rich porphyrin groups in HRP; the second one is the hydrogen bonding between the amino groups of ABEI and the carboxyl group of HRP; and the third one is the electrostatic interaction between positively charged HRP and negatively charged oxidation product of ABEI. Therefore, the possible assembling mechanism of ABEI-GO@HRP has been proposed as follows: ABEI molecules were first functionalized on the surface of GO via $\pi-\pi$ interaction. On the one hand, HRP as a catalyst was also directly assembled on the surface of GO by electrostatic interaction, and ABEI and HRP covered both sides of GO. On the other hand, HRP was connected to ABEI molecules to form an HRP/ABEI/GO/ABEI/HRP structure by virtue of $\pi-\pi$ stacking and hydrogen bonding.

CONCLUSIONS

A novel hybrid material, ABEI-GO@HRP, has been successfully synthesized through a facile and green synthesis process. In this strategy, ABEI molecules were first attached on the surface of GO via $\pi-\pi$ interactions to form ABEI-GO. Then HRP as a catalyst was assembled on the GO-based composites, probably in two ways. HRP may be directly assembled on the

Table 2. Determination of H_2O_2 Concentration in Human Urine Samples

urine samples	H_2O_2 detected (mean ± σ, n = 3) (nM)	H_2O_2 added (nM)	total H_2O_2 detected (mean ± σ, n = 3) (nM)	recovery (%)
1	2.17 ± 0.12	10	12.24 ± 0.31	103.23
2	4.89 ± 0.20	10	14.73 ± 0.42	96.72
3	3.14 ± 0.06	10	13.11 ± 0.31	99.04

DOI: 10.1021/acsami.5b05325
ACS Appl. Mater. Interfaces 2015, 7, 18283−18291

surface of GO by strong electrostatic interaction. HRP might also be immobilized on the surface of ABEI-GO using ABEI as a bridge molecule to form HRP/ABEI/GO/ABEI/HRP structure by virtue of $\pi-\pi$ stacking and hydrogen bonding. The ABEI-GO@HRP hybrids were easily purified by centrifugation, which is much simpler and faster than the purification of ABEI and hemin bifunctionalized graphene hybrids. The obtained ABEI-GO@HRP hybrids exhibited excellent CL activity in neutral and alkaline conditions when reacted with H_2O_2, which is superior to that of the previously reported ABEI functionalized graphene composites as well as ABEI and hemin bifunctionalized graphene hybrids. Such strong CL emission of ABEI-GO@HRP hybrids was probably due to the overlying peroxidase-property of HRP and GO which could facilitate the formation of $O_2^{\bullet-}$, $-CO_4^{\bullet 2-}$, $HO^{\bullet}$, and π-C=C$^{\bullet}$ in the CL reaction, and GO as a reaction platform promoted the radical-involved redox reaction. ABEI-GO@HRP could be directly used as a platform for sensing of H_2O_2. It is ultrasensitive, selective, and reagentless. Attributing to excellent catalytic activity and enzymatic specificity of HRP, the sensitivity and selectivity of the presented sensor is superior to that of previously reported H_2O_2 assays. This work provides an effective tool for the determination of H_2O_2 in neutral and alkaline conditions. Moreover, CL emission of ABEI-GO@HRP hybrids in physiological conditions is even more than 1 order of magnitude stronger than that of ABEI-GO in optimal alkaline pH, which may find future applications under physiological conditions, such as biological imaging, the detection of reactive oxygen species in cell and cancer diagnosis. Taking advantage of excellent CL property, enzyme specificity, solubility, and biocompatibility, ABEI-GO@HRP hybrids may be used as ideal platforms and probes for the design of new bioassays and biosensors. In addition, this study may be extended to the synthesis of other GO hybrids bifunctionalized by other peroxidases and CL reagents via a simple synthesis.

■ ASSOCIATED CONTENT

Supporting Information

The Supporting Information is available free of charge on the ACS Publications website at DOI: 10.1021/acsami.5b05325.

Additional information as noted in text, including FT-IR, CD, and TEM characterization of ABEI-GO@HRP, a CL comparison for reaction of ABEI, ABEI + GO, ABEI + HRP, ABEI + GO@HRP, ABEI-GO@HRP with H_2O_2, optimization for synthetic conditions of ABEI-GO@HRP and CL reaction conditions of ABEI-GO@HRP with H_2O_2 and interaction study between ABEI and HRP by fluorescence and UV−vis spectra (PDF)

■ AUTHOR INFORMATION

Corresponding Author

* Tel: +86-551-63600730; fax: +86-551-63600730; e-mail: hcui@ustc.edu.cn.

Notes

The authors declare no competing financial interest.

■ ACKNOWLEDGMENTS

The support of this research by the National Natural Science Foundation of PR China (Grant Nos. 21475120 and 21173201) and the Opening Fund of State Key Laboratory of Electroanalytical Chemistry, Changchun Institute of Applied Chemistry, CAS (Grant No. SKLEAC201408) are gratefully acknowledged.

■ REFERENCES

(1) Li, D.; Muller, M. B.; Gilje, S.; Kaner, R. B.; Wallace, G. G. Processable Aqueous Dispersions of Graphene Nanosheets. *Nat. Nanotechnol.* **2008**, *3*, 101−105.

(2) Park, S.; Ruoff, R. S. Chemical Methods for The Production of Graphenes. *Nat. Nanotechnol.* **2009**, *4*, 217−224.

(3) Tung, V. C.; Allen, M. J.; Yang, Y.; Kaner, R. B. High-throughput Solution Processing of Large-scale Graphene. *Nat. Nanotechnol.* **2009**, *4*, 25−29.

(4) Shen, J.; Hu, Y.; Shi, M.; Lu, X.; Qin, C.; Li, C.; Ye, M. Fast and Facile Preparation of Graphene Oxide and Reduced Graphene Oxide Nanoplatelets. *Chem. Mater.* **2009**, *21*, 3514−3520.

(5) Liu, Y.; Yu, D.; Zeng, C.; Miao, Z.; Dai, L. Biocompatible Graphene Oxide-Based Glucose Biosensors. *Langmuir* **2010**, *26*, 6158−6160.

(6) Dreyer, D. R.; Park, S.; Bielawski, C. W.; Ruoff, R. S. The Chemistry of Graphene Oxide. *Chem. Soc. Rev.* **2010**, *39*, 228−240.

(7) Chen, D.; Feng, H.; Li, J. Graphene Oxide: Preparation, Functionalization, and Electrochemical Applications. *Chem. Rev.* **2012**, *112*, 6027−6053.

(8) Shen, W.; Yu, Y.; Shu, J.; Cui, H. A Graphene-based Composite Material Noncovalently Functionalized with a Chemiluminescence Reagent: Synthesis and Intrinsic Chemiluminescence Activity. *Chem. Commun.* **2012**, *48*, 2894−2896.

(9) He, Y.; Cui, H. Fabrication of Luminol and Lucigenin Bifunctionalized Gold Nanoparticles/Graphene Oxide Nanocomposites with Dual-Wavelength Chemiluminescence. *J. Phys. Chem. C* **2012**, *116*, 12953−12957.

(10) He, Y.; Cui, H. Synthesis of Dendritic Platinum Nanoparticles/Lucigenin/Reduced Graphene Oxide Hybrid with Chemiluminescence Activity. *Chem. - Eur. J.* **2012**, *18*, 4823−4826.

(11) He, Y.; Cui, H. Synthesis of Highly Chemiluminescent Graphene Oxide/Silver Nanoparticle Nano-composites and their Analytical Applications. *J. Mater. Chem.* **2012**, *22*, 9086−9091.

(12) Liu, D.; Huang, G.; Yu, Y.; He, Y.; Zhang, H.; Cui, H. N-(Aminobutyl)-N-(ethylisoluminol) and Hemin Dual-functionalized Graphene Hybrids with High Chemiluminescence. *Chem. Commun.* **2013**, *49*, 9794−9796.

(13) Pavlov, V.; Xiao, Y.; Gill, R.; Dishon, A.; Kotler, M.; Willner, I. Amplified Chemiluminescence Surface Detection of DNA and Telomerase Activity using Catalytic Nucleic Acid Labels. *Anal. Chem.* **2004**, *76*, 2152−2156.

(14) Freeman, R.; Liu, X.; Willner, I. Chemiluminescent and Chemiluminescence Resonance Energy Transfer (CRET) Detection of DNA, Metal Ions, and Aptamer−substrate Complexes using Hemin/G-quadruplexes and CdSe/ZnS Quantum Dots. *J. Am. Chem. Soc.* **2011**, *133*, 11597−11604.

(15) Liu, X.; Freeman, R.; Golub, E.; Willner, I. Chemiluminescence and Chemiluminescence Resonance Energy Transfer (CRET) Aptamer Sensors using Catalytic Hemin/G-quadruplexes. *ACS Nano* **2011**, *5*, 7648−7655.

(16) Bornscheuer, U. T. Immobilizing Enzymes: How to Create More Suitable Biocatalysts. *Angew. Chem., Int. Ed.* **2003**, *42*, 3336−3337.

(17) Zhang, J.; Zhang, F.; Yang, H.; Huang, X.; Liu, H.; Zhang, J.; Guo, S. Graphene Oxide as a Matrix for Enzyme Immobilization. *Langmuir* **2010**, *26*, 6083−6085.

(18) Zhang, Y.; Zhang, J.; Huang, X.; Zhou, X.; Wu, H.; Guo, S. Assembly of Graphene Oxide−enzyme Conjugates through Hydrophobic Interaction. *Small* **2012**, *8*, 154−159.

(19) Zhang, F.; Zheng, B.; Zhang, J.; Huang, X.; Liu, H.; Guo, S.; Zhang, J. Horseradish Peroxidase Immobilized on Graphene Oxide: Physical Properties and Applications in Phenolic Compound Removal. *J. Phys. Chem. C* **2010**, *114*, 8469−8473.

(20) Zhang, Q.; Yang, S.; Zhang, J.; Zhang, L.; Kang, P.; Li, J.; Xu, J.; Zhou, H.; Song, X. M. Fabrication of an Electrochemical Platform

DOI: 10.1021/acsami.5b05325
ACS Appl. Mater. Interfaces 2015, 7, 18283−18291

Based on the Self-assembly of Graphene Oxide−multiwall Carbon Nanotube Nanocomposite and Horseradish Peroxidase: Direct Electrochemistry and Electrocatalysis. *Nanotechnology* **2011**, *22*, 494010.
(21) Zhang, Y.; Wu, C.; Guo, S.; Zhang, J. Interactions of Graphene and Graphene Oxide with Proteins and Peptides. *Nanotechnol. Rev.* **2013**, *2*, 27−45.
(22) Wang, Q.; Kromka, A.; Houdkova, J.; Babchenko, O.; Rezek, B.; Li, M.; Boukherroub, R.; Szunerits, S. Nanomolar Hydrogen Peroxide Detection using Horseradish Peroxidase Covalently Linked to Undoped Nanocrystalline Diamond Surfaces. *Langmuir* **2012**, *28*, 587−592.
(23) Jia, N.; Zhou, Q.; Liu, L.; Yan, M.; Jiang, Z. Direct Electrochemistry and Electrocatalysis of Horseradish Peroxidase Immobilized in Sol−gel-derived Tin Oxide/gelatin Composite Films. *J. Electroanal. Chem.* **2005**, *580*, 213−221.
(24) Li, T.; Park, H. G.; Lee, H. S.; Choi, S. H. Circular Dichroism Study of Chiral Biomolecules Conjugated with Silver Nanoparticles. *Nanotechnology* **2004**, *15*, S660.
(25) Gao, L.; Zhang, H.; Cui, H. A General Strategy to Prepare Homogeneous and Reagentless GO/lucigenin&enzyme Biosensors for Detection of Small Biomolecules. *Biosens. Bioelectron.* **2014**, *57*, 65−70.
(26) Stankovich, S.; Dikin, D. A.; Piner, R. D.; Kohlhaas, K. A.; Kleinhammes, A.; Jia, Y.; Wu, Y.; Nguyen, S. T.; Ruoff, R. S. Synthesis of Graphene-based Nanosheets via Chemical Reduction of Exfoliated Graphite Oxide. *Carbon* **2007**, *45*, 1558−1565.
(27) McAllister, M. J.; Li, J. L.; Adamson, D. H.; Schniepp, H. C.; Abdala, A. A.; Liu, J.; Herrera Alonso, M.; Milius, D. L.; Car, R.; Prud'homme, R. K. Single Sheet Functionalized Graphene By Oxidation and Thermal Expansion of Graphite. *Chem. Mater.* **2007**, *19*, 4396−4404.
(28) Thorpe, G. H.; Kricka, L. J. Enhanced Chemiluminescent Reactions Catalyzed by Horseradish Peroxidase. *Methods Enzymol.* **1986**, *133*, 331−353.
(29) Zhang, Z. F.; Cui, H.; Lai, C. Z.; Liu, L. J. Gold Nanoparticle-catalyzed Luminol Chemiluminescence and Its Analytical Applications. *Anal. Chem.* **2005**, *77*, 3324−3329.
(30) Li, F.; Liu, Y.; Zhuang, M.; Zhang, H.; Liu, X.; Cui, H. Biothiols as Chelators for Preparation of N-(aminobutyl)-N-(ethylisoluminol)/Cu^{2+} Complexes Bifunctionalized Gold Nanoparticles and Sensitive Sensing of Pyrophosphate Ion. *ACS Appl. Mater. Interfaces* **2014**, *6*, 18104−18111.
(31) Thorpe, G. H.; Kricka, L. J. Enhanced Chemiluminescent Reactions Catalyzed by Horseradish Peroxidase. *Methods. Enzymol.* **1986**, *133*, 331−353.
(32) Nakamura, M.; Nakamura, S. One and Two-electron Oxidations of Luminol by Peroxidase Systems. *Free Radical Biol. Med.* **1998**, *24*, 537−544.
(33) Liu, M.; Zhang, H.; Shu, J.; Liu, X.; Li, F.; Cui, H. Gold Nanoparticles Bifunctionalized by Chemiluminescence Reagent and Catalyst Metal Complexes: Synthesis and Unique Chemiluminescence Property. *Anal. Chem.* **2014**, *86*, 2857−2861.
(34) Wang, Y.; Lu, J.; Tang, L.; Chang, H.; Li, J. Graphene Oxide Amplified Electrogenerated Chemiluminescence of Quantum Dots and its Selective Sensing for Glutathione from Thiol-containing Compounds. *Anal. Chem.* **2009**, *81*, 9710−9715.
(35) Nandini, S.; Nalini, S.; Manjunatha, R.; Shanmugam, S.; Melo, J. S.; Suresh, G. S. Electrochemical Biosensor for the Selective Determination of Hydrogen Peroxide Based on the Co-deposition of Palladium, Horseradish Peroxidase on Functionalized-graphene Modified Graphite Electrode as Composite. *J. Electroanal. Chem.* **2013**, *689*, 233−242.
(36) Wang, D. M.; Zhang, Y.; Zheng, L. L.; Yang, X. X.; Wang, Y.; Huang, C. Z. Singlet Oxygen Involved Luminol Chemiluminescence Catalyzed by Graphene Oxide. *J. Phys. Chem. C* **2012**, *116*, 21622−21628.
(37) Misra, H. P.; Squatrito, P. M. The Role of Superoxide Anion in Peroxidase-catalyzed Chemiluminescence of Luminol. *Arch. Biochem. Biophys.* **1982**, *215*, 59−65.
(38) Yang, L.; Zhang, R.; Liu, B.; Wang, J.; Wang, S.; Han, M. Y.; Zhang, Z. π-Conjugated Carbon Radicals at Graphene Oxide to Initiate Ultrastrong Chemiluminescence. *Angew. Chem., Int. Ed.* **2014**, *53*, 10109−10113.
(39) Yuan, L.; Lin, W.; Xie, Y.; Chen, B.; Zhu, S. Single Fluorescent Probe Responds to H_2O_2, NO, and H_2O_2/NO with Three Different Sets of Fluorescence Signals. *J. Am. Chem. Soc.* **2012**, *134*, 1305−1315.
(40) Winterbourn, C. C. Reconciling the Chemistry and Biology of Reactive Oxygen Species. *Nat. Chem. Biol.* **2008**, *4*, 278−286.
(41) Murphy, M. P.; Holmgren, A.; Larsson, N. G.; Halliwell, B.; Chang, C. J.; Kalyanaraman, B.; Rhee, S. G.; Thornalley, P. J.; Partridge, L.; Gems, D. Unraveling the Biological Roles of Reactive Oxygen Species. *Cell Metab.* **2011**, *13*, 361−366.
(42) Lin, M. T.; Beal, M. F. Mitochondrial Dysfunction and Oxidative Stress in Neurodegenerative Diseases. *Nature* **2006**, *443*, 787−795.
(43) Nishikawa, M. Reactive Oxygen Species in Tumor Metastasis. *Cancer Lett.* **2008**, *266*, 53−59.
(44) Rubtsova, M. Y.; Kovba, G. V.; Egorov, A. M. Chemiluminescent Biosensors Based on Porous Supports with Immobilized Peroxidase. *Biosens. Bioelectron.* **1998**, *13*, 75−85.
(45) Lyon, J. L.; Stevenson, K. J. Picomolar Peroxide Detection Using a Chemically Activated Redox Mediator and Square Wave Voltammetry. *Anal. Chem.* **2006**, *78*, 8518−8525.
(46) Wen, F.; Dong, Y.; Feng, L.; Wang, S.; Zhang, S.; Zhang, X. Horseradish Peroxidase Functionalized Fluorescent Gold Nanoclusters for Hydrogen Peroxide Sensing. *Anal. Chem.* **2011**, *83*, 1193−1196.
(47) Ali, M.; Tahir, M. N.; Siwy, Z.; Neumann, R.; Tremel, W.; Ensinger, W. Hydrogen Peroxide Sensing with Horseradish Peroxidase-Modified Polymer Single Conical Nanochannels. *Anal. Chem.* **2011**, *83*, 1673−1680.
(48) Peng, Y.; Jiang, D.; Su, L.; Zhang, L.; Yan, M.; Du, J.; Lu, Y.; Liu, Y. N.; Zhou, F. Mixed Monolayers of Ferrocenylalkanethiol and Encapsulated Horseradish Peroxidase for Sensitive and Durable Electrochemical Detection of Hydrogen Peroxide. *Anal. Chem.* **2009**, *81*, 9985−9992.
(49) Zhiguo, G.; Shuping, Y.; Zaijun, L.; Xiulan, S.; Guangli, W.; Yinjun, F.; Junkang, L. An Ultrasensitive Hydrogen Peroxide Biosensor Based on Electrocatalytic Synergy of Graphene−gold Nanocomposite, CdTe−CdS Core−shell Quantum Dots and Gold Nanoparticles. *Anal. Chim. Acta* **2011**, *701*, 75−80.
(50) Kuge, N.; Kohzuki, M.; Sato, T. Relation Between Natriuresis and Urinary Excretion of Hydrogen Peroxide. *Free Radical Res.* **1999**, *30*, 119−123.
(51) Chatterjee, S.; Chen, A. Functionalization of Carbon Buckypaper for the Sensitive Determination of Hydrogen Peroxide in Human Urine. *Biosens. Bioelectron.* **2012**, *35*, 302−307.

DOI: 10.1021/acsami.5b05325
ACS Appl. Mater. Interfaces 2015, 7, 18283−18291